Title: INFLUENCE OF THE GEOMETRICAL DESIGN ON BALL AND CROSSED ROLLER WIRE RACE BEARING BEHAVIOR UNDER AXIAL LOAD

Authors: Iñigo Martín[1], Iker Heras[1], Josu Aguirrebeitia[1], Luis María Macareno[1]

1 Department of Mechanical Engineering, Faculty of Engineering Bilbao, University of the Basque Country (UPV/EHU), Plaza Ingeniero Torres Quevedo, 1, 48013, Bilbao, Spain.

* Corresponding author:
Iñigo Martín
E-mail address: inigo.martin@ehu.eus
Tel.: +0034 606 061 117

Abstract

Wire bearings are becoming popular these days in applications such as defence, robotics, medical devices or shipping industry. They provide weight and inertia reductions, good shock load and vibration absorbing capacity, constant torque and low maintainance. Despite all the benefits of this kind of bearings, there are few wire race bearing manufacturers, which own the design and manufacturing know-how. This work is focused on providing some design guidelines for ball and crossed roller wire race bearings established upon different geometrical parameters, by means of a DoE performed with Finite Element simulations. The results of the simulations are carefully compared to obtain the effects of those geometrical parameters in several performance indicators.

Keywords

Wire Race Bearing; Slewing Bearing; Bearing Design; Bearing Stiffness

1. Introduction

Wire race slewing bearings are a special kind of bearings. On the one hand, their cross-section is characteristic for having a mean diameter far greater than the rolling element diameter. On the other hand, rolling elements run over wires with machined raceways placed between the rolling elements and the rings. There are several types of wire race bearings, being the four point contact ball bearings and crossed roller bearings two of the most popular ones; they are represented and labeled in Fig. 1.

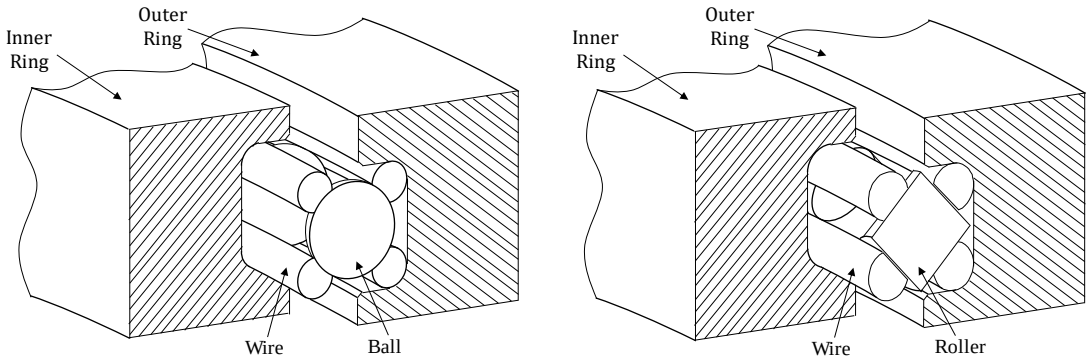

(a) (b)

Fig. 1. Wire race bearing cross-section: (a) Ball (b) Roller

Slewing bearings can face large axial and radial loads, as well as tilting moments, and they are mainly used for orientation purposes. Rolling elements and wires must be wear-resistant since they suffer rolling contact, for that reason, they are manufactured in hardened steel. Therefore, several possibilities arise when choosing the ring material, where aluminium, bronze, carbon fiber or plastic are available. According to manufacturers, aluminium can retrieve significant weight savings (up to 65% [1]) and improvements in some performance indicators. Lower mass and inertia make these bearings appropriate for applications as robotics and aerospace. A lower elastic modulus and the existence of more contact interfaces than in conventional bearings, provide a good shock load and travelling vibrations absorbing capacity, thus better at avoiding race damage [2]. For that reason, they are employed in medical devices, defence applications or shipping industry, where vibrations and shock loads are a common issue. Wires are not closed circumferencially; they have a cut with a gap, which eases the assembly process and acts as expansion gap; this means that friction torque remains constant with temperature variations [3].

The manufacturing process is not straightforward due to the inherent difficulty of bending the hardened wires. For that reason, there are only a few manufacturers and almost all the know-how is in their hands. Nevertheless, some research in this area has been carried out in recent years to provide knowledge to customers and potential manufacturers. Regarding structural behaviour, Gunia and Smolnicki developed

two research works. The first one studied the influence of certain geometrical parameters in the ball-wire contact stress distribution [4]. In the second one they proposed a corrected wire-raceway geometry for ball wire race bearings that reduces the free edge stress concentration effect [5]. Martin et al. studied the behaviour and the influence of some design parameters in ball wire race bearings under axial load, explaining the wire-twisting phenomenon and comparing the results with equivalent conventional bearings [6]. In terms of analytical models, Shan et al. proposed an analytical method to obtain the preload in ball wire race bearings with non-conformal ball-wire contact [7]. Later, Aguirrebeitia et al. developed a formula to obtain the wire twisting stiffness of the race shaped wires [8]. Martin et al. developed two works related to analytical tools: in [9] they present an analytical model to estimate the stiffness and contact results of a ball wire race bearing under axial load, and in [10] they proposed a semi-analytical modelization of the roller-wire-ring submodel with the aim of implementing it in a Finite Element (FE) model and improving the computational efficiency in static structural analyses.

Due to the recency of works regarding wire race bearings, some insight becomes necessary when an engineer faces the design problem. Therefore, knowing the influence of design parameters in the performance of the bearings is a neccesary step to optimize the design. In this sense, this work presents a study of the effects of several geometrical parameters on the performance under axial load. The results were obtained by means of FE simulations within a Design of Experiments (DoE) for both ball and roller wire race bearings. The most relevant results are graphically displayed with explanations about the main effects of the design parameters on different performance indicators.

2. Methodology

For this work, a deep study of several manufacturers' catalogues of wire race ball bearings (ball bearings from now on) and crossed roller wire race bearings (roller bearings from now on) was carried out to identify the most representative geometrical parameters and define the design space of the DoEs. Finally, a FE simulation for each design point retrieves the main and crossed effects of the geometrical parameters in the performance indicators.

2.1. Design parameters definition

Fig. 2 shows the geometrical parameters for both bearing geometries. There appear many different parameters, but performing a DoE with all of them would lose significance; for that reason, only the most relevant design parameters related with the geometry of the contact areas were considered in this work. Bearing mean diameter (D_{pw}) and the initial contact angle (α_0) remained constant because their effects are already known from studies in conventional bearings. Besides, D_{pw} is usually dependant on the application and cannot be modified. The length of the rollers was also not considered as design parameter, because in crossed roller wire race bearings, it is always larger than the raceway width; this means that roller length does not affect the roller-raceway contact area.

In order to obtain general results, the DoE parameters were chosen non-dimensional or dependant on the rolling element diameter (D_w). This rolling element diameter is the first parameter to be considered, because it states the size of the cross section and the number of rolling elements (N). Besides, to study the influence of the wire diameter (λ), the non-dimensional parameter λ_r was defined, where $\lambda_r=\lambda/D_w$. Regarding the size of the raceway, another non-dimensional parameter called raceway factor (Rf) was created. Eq. 1 defines Rf in terms of the parameters of the DoE, where D_{cw} is the diameter of the circumference that connects the center of the wires (see Fig. 2). This parameter indicates how much wire material is machined to create the raceway, in such a way that Rf=0 ($D_w+\lambda=D_{cw}$) means that no material is machined (the contact between wire and rolling element becomes non-conformal) and Rf=1 means that half of the wire section is removed ($D_w=D_{cw}$).

$$Rf = \frac{\lambda + D_w - D_{cw}}{\lambda} = 1 + \frac{1}{\lambda/D_w} - \frac{1}{\lambda/D_{cw}} \quad (1)$$

Apart from the three parameters defined above, the osculation ratio (s) in Eq. 2 is a relevant parameter for ball bearings since it expresses the conformity of the ball-wire contact:

$$s = \frac{D_w}{2 \cdot R_c} \tag{2}$$

where R_c is the raceway groove radius. Regarding the dimensions of the cross section of the ring, it was considered unaproppiate to keep it constant for all cases, since the size of the cross section of the ring is usually related to the rolling element diameter D_w for regular bearings. The work developed by Heras in [11], proposed a general crossed section geometry for conventional bearings, dependant on D_w and the coeficients R_L, R_H, R_{Lg}, which were obtained from a deep study of catalogue geometries (see Fig. 2). For the present study the same coefficients were used but dependant on the size of the housing (H) instead of doing it dependant on D_w. Table 1 shows ring coefficients together with the constant geometry parameters. R is the radius of the wire housing, and its value is the radius of the wire minus 0.1 [mm] [12]. A 100% fill factor [11] indicates that the maximum allowable number of rolling elements were considered. Constant fill factor and constant D_{pw} also mean that the number of rolling elements varies if D_w changes. Summarizing, the design parameters considered were s, D_w, λ_r and Rf for ball bearings, and D_w, λ_r and Rf for roller bearings.

Table 1
Ring coefficients and constant geometry parameters

D_{pw}	α_0	*Fill Factor*	R_L	R_H	R_{Lg}	H_g
420 [mm]	45 [deg]	100[%]	1.9	2.15	0.1	3 [mm]

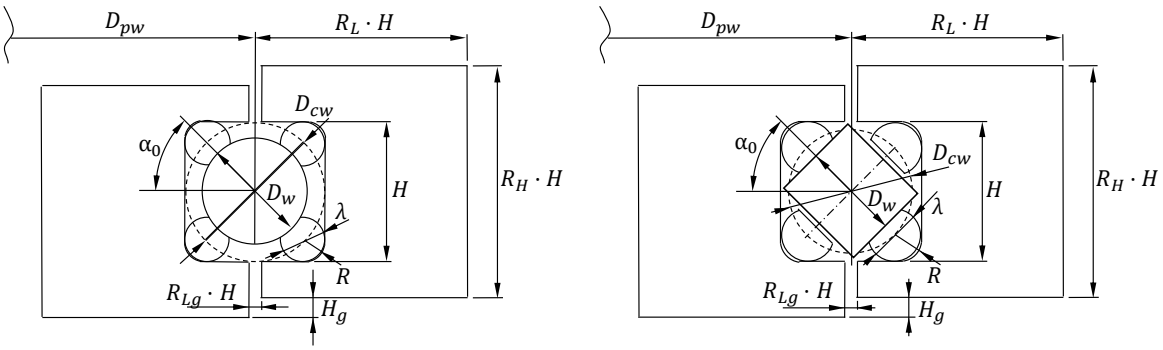

Fig. 2. Geometrical parameters: (a) Ball (b) Roller

2.2. Design of Experiments

A 2 level full factorial design was considered to assess overall main and crossed effects, from which pareto diagrams are built. In addition, some design points were added to account for nonlinearities and to simplify postprocessing, resulting in 25 design points for ball bearings and 15 for roller bearings. The ranges of the geometrical parameters that appear in the matrices of experiments were defined from values found in commercial catalogues.

Fig. 3 shows the matrices of experiments for both bearing types with a color code to indicate the purpose of each design point. Green points are those regarding the 2 level full factorial design. Black point corresponds to the reference geometry for each bearing and it acts as midpoint to account for possible nonlinearities in main effects. And last, red design points represent geometries where the main effects can be independently analyzed and observed.

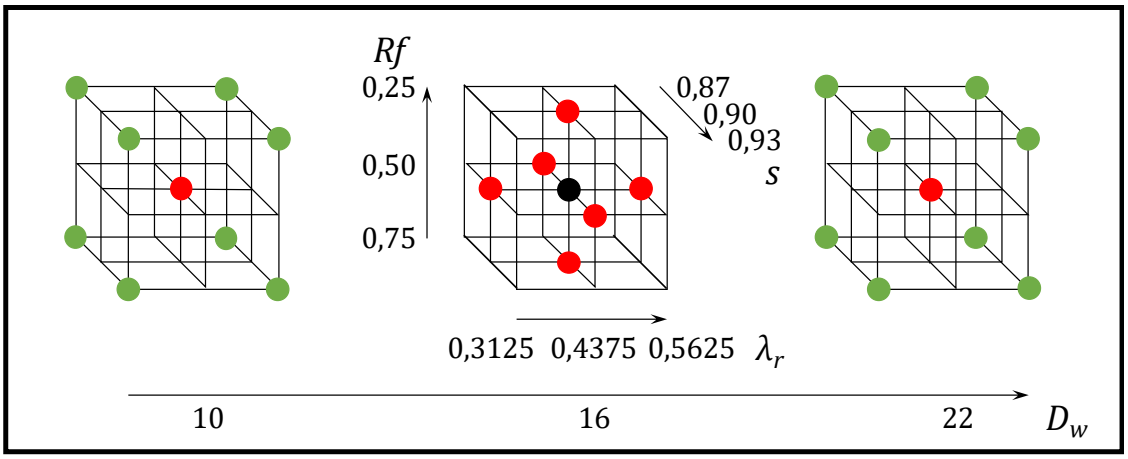

(a)

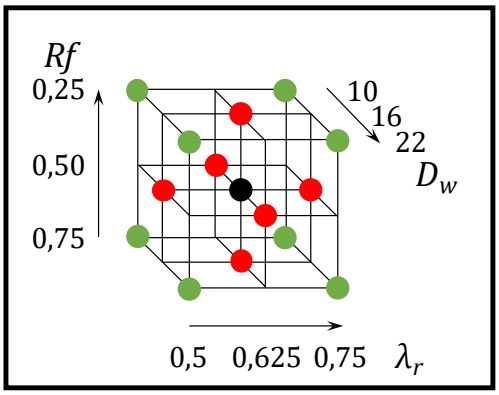

(b)

Fig. 3. Matrix of experiments: (a) Ball bearings (b) Roller bearings

2.3. Finite Element Models

The purpose of this work is to study the influence of some relevant geometrical parameters in the performance of wire race bearings under axial load. To obtain the results, two parametric FE models were created in Ansys®, represented with the reference geometry values in Fig. 4. Since load and geometry are cyclic symmetric, only one sector model with half a ball is enough for ball bearings, and one sector model with two roller halves is enough for roller bearings. Structural steel (E=200 [GPa]) was assigned for rolling elements and wires, and aluminium (E=71 [GPa]) for the rings, since it is a common layout in most applications. Both materials were assumed to be linear elastic, so local permanent deformations cannot be obtained. Moreover, chamfers or eventual roller crowning were not considered in the FE models, and neither were wire edge fillets, since there is no standard geometry for the wires so far. This can lead to non-realistic results in local stress concentration areas and truncated pressure patches. Nevertheless, the effect in the stress distribution of wire edge geometry correction by the addition of a fillet was studied by Gunia in [5]**.** As a result of that study, they observed that the geometry correction reduced the stress concentrations due to edge effects, but the behaviour of the rest of the contact did not change significantly. This reduction of the stress concentration has important implications in bearing fatigue behavior, but does not affect the global behavior of the contact, and therefore neither does the response of the bearing in terms of load distribution or global deflections. Consequently, the FE model will predict when the contact reaches the limits of the raceway, but can not calculate the real stress peak. These areas are quite local and good results can be obtained at a certain distance from them.

In order to obtain a proper mesh, some partitions were carried out in the geometry that allow to mesh different volumes of the same component with different mesh sizes or element types. Fig. 4 shows that the contact zones are meshed with second order hexaedrons with a small element size (0.3 [mm]), while zones far away of the contact are meshed with second order tethaedrons that retrieves faster size transitions to bigger elements preserving a good aspect ratio. The DoF of the model changes from one case to another

depending on the value of the geometrical paremeters, but the total number is always around 1,500,000 DoF for both bearing types.

Contacts are grease lubricated, so they were defined as frictional according to the Coulomb model, with a coefficient of friction of 0.1 [13–15]. An Augmented Lagrange formulation was used, letting the program automatically control the normal contact stiffness and updating it each iteration in order to achieve a maximum mesh penetration of 1 [μm] (penetration tolerance).

While boundary conditions usually depend on the application or the surrounding structures, this work pretends to be generalistic and aims to study the local behaviour of the component. In this sense, rigid boundary conditions were imposed to the external faces of the rings and a external axial displacement was applied to those faces to reach the static load carrying capacity provided by the methodology developed in [16] for ball bearings and in [17] for roller bearings. Symmetry boundary conditions were also applied to the cyclic symmetric faces.

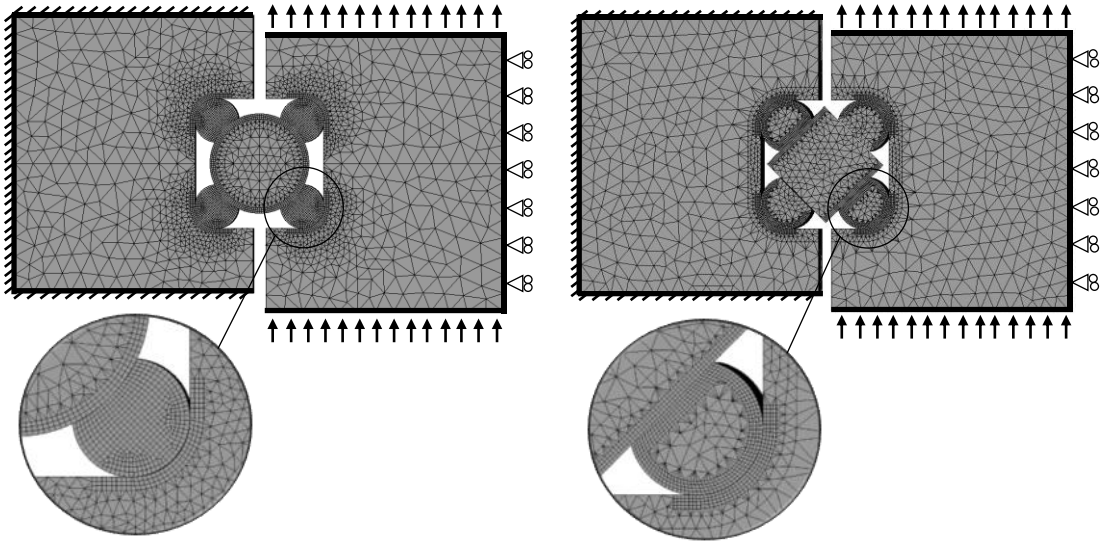

(a) (b)

Fig. 4. FE models: (a) Ball bearing (b) Roller bearing

2.4. Performance Indicators

In order to assess the influence of the geometrical design parameters in the performance of the bearing, some indicators must be used. Those indicators should properly represent the structural behaviour and the capability of the bearing to face external loads.

- Axial static load capacity (C_{0a}). The axial static load capacity can be analytically obtained [16,17] and retrieves the maximum axial load that the contact between rolling element and raceway can bear until a permanent deformation of one 10,000th of the rolling element diameter arises, according to ISO-76 [18]; in that standard, the maximum allowable force is the one that generates a contact pressure of 4200 [MPa] for ball bearings and 4000 [MPa] for roller barings, calculated with Hertz's elastic contact theory. Although this way for defining the capacity of a bearing to face external loads may be insufficient for some applications and operating modes (it does not account for fatigue, core crushing and other damage sources), it can be perfectly used as a load capacity indicator with comparative purposes.
- Stiffness. Axial stiffness can be defined as the response of the bearing in terms of deformation under an applied axial force. It is usually represented with axial force/axial deformation curves. In order to define an "overall stiffness constant" to represent those curves, the force-to-deformation ratio is calculated for a given value of the force, common for all of them.
- Wire twist. This phenomenon may not be considered directly as a performance indicator, but it has a significant contribution to the understanding of the performance of the bearing, as it will be observed in following sections. Wire twist arises when the bearing is loaded because the contact

force exerts a twisting moment [6]. This phenomenon turns beneficial since, this way, the ball-wire contact tends to remain centered within the raceway thus preventing early contact patch truncation and allowing the wires-roller set behave as a single solid. The twist angle varies with the axial deformation and it can be represented by means of twist angle/axial deformation curves. In order to define an "overall wire twist" to represent those curves, the maximum twist angle variation may be reported for a given value of axial deformation, common for all of them.

- Contact angle. It is the angle between the radial plane and the normal force vector sum of the rolling element-wire contact. The variation of this angle comes from phenomena such as ball climbing (only in ball bearings) and wire twisting [6], and it is an indicator of the position of the contact. The knowledge of the variation of this indicator retrieves valuable information of the behaviour of the bearing for its analytical modelling. Contact angle variation has also a significant contribution to the stiffness curve: it would be almost linear in case this variation does not exist. The contact angle varies with the axial deformation and it can be represented by means of contact angle/axial deformation curves. In order to define an "overall contact angle" to represent those curves, the maximum contact angle variation may be reported for a given value of axial deformation, common for all of them.
- Contact pressure contours. Finally, the pressure lines are presented along the major axis of the ball-wire contact ellipse for ball bearings and the roller-wire contact rectangle for roller bearings during the loading process. Five load levels are represented equally spaced until the maximum applied load and the raceway limits are marked with vertical lines. The objective of these plots is twofold: assess whether the existing methodologies are able to correctly predict the axial static capacity, and detect the occurrence of contact patch truncation, which would involve a pressure increase above the theoretically calculated one, as well as dangerous overstresses. As it has been previously stated, the FE models used in this work are not able to predict the real behavior in the stress concentration areas, but they provide good results in the rest of the contact in order to achieve the aforementioned objectives.

3. Results

Once carried out the Finite Element analyses detailed in the DoE, the performance indicators for both ball and roller bearings are explained in separate sections as functions of the design parameters. Each section starts with explanations about the relative weight of the main effects of each design parameter and the crossed effects among them on the overall values of the performance indicators. Crossed effects can have a significative influence in the performance indicators; a study of those crossed effects is necessary to ensure whether the conclusions obtained from the analysis of the main effects are enough or not. Then, those main effects are analyzed for each performance indicator and finally, a brief summary of the main effects is presented.

3.1. Ball Bearings

Previous considerations

Fig. 5 shows a summary of the main and crossed effects of the design parameters on the overall values of the performance indicators, where the summation of main and crossed effects equals 100%. It can be observed that crossed effects do not affect too much the axial static load capacity and the stiffness, with a cummulative effect of a 12% and a 20% respectively. The summation of the crossed effects for the wire twist reaches a 27%, which is also relatively low. Regarding the contact angle variation, the cumulative weight of the crossed effects rises up to 41%; this reveals that the influence of the design parameters is diffuse and this can be, in part, due to the inherent difficulty of establishing a proper overall value to represent the contact angle variation with an overall value.

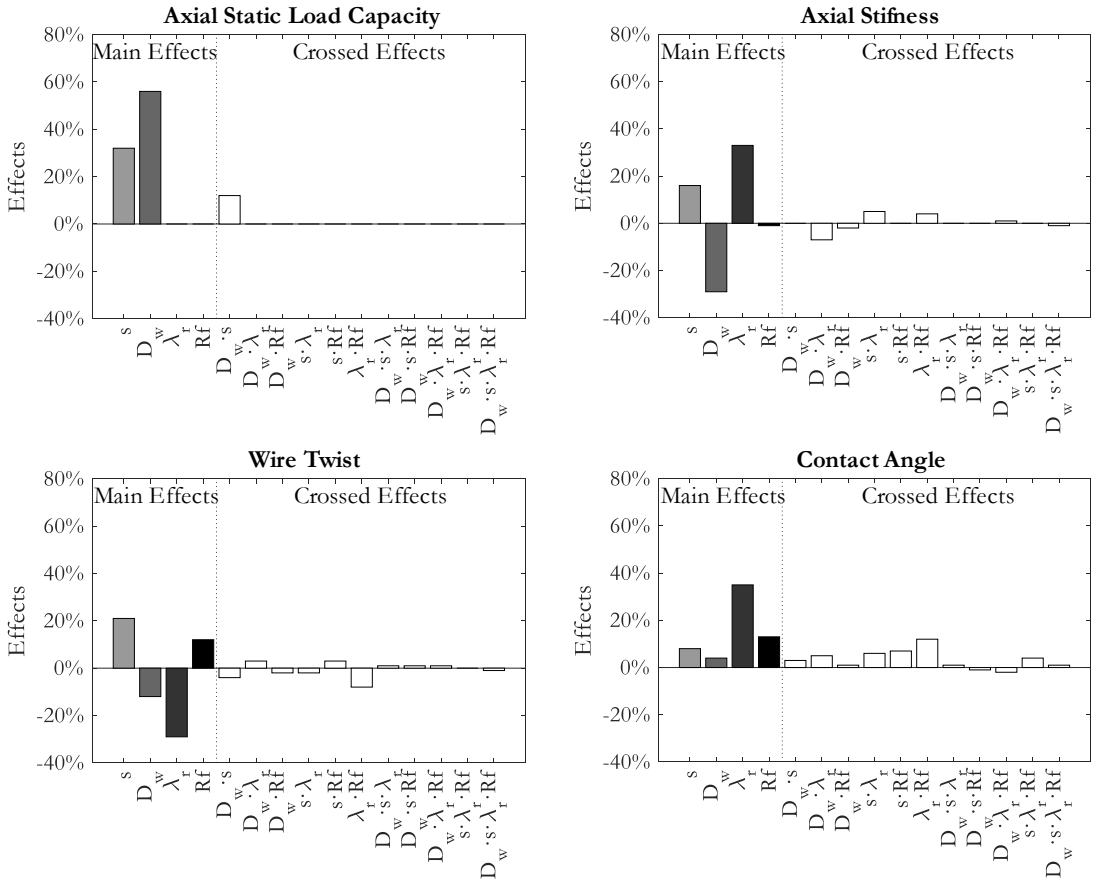

Fig. 5. Ball bearing main and crossed effects

Axial Static Load Capacity

In this section, the axial static load capacity according to ISO-76 standard is compared. The effect of the contact ellipse truncation can not be evaluated with this method but will be observed later in this section. The axial static load capacity is a parameter that can be altered by changes in osculation ratio *s* or in ball diameter D_w as it can be observed in Fig. 6. A more conformal contact is able to bear more load before reaching the maximum allowable contact pressure; the same happens with a bigger ball diameter, but it must be taken into account that a bigger diameter involves a lower number of rolling elements. λ_r and *Rf* do not apparently affect to the capacity, because they do not modify the geometry of the contact.

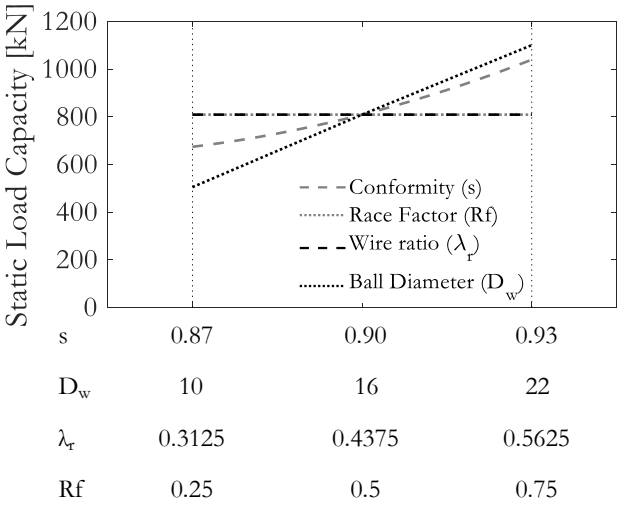

Fig. 6. Ball bearing axial static load capacity

Axial Stiffness

Fig. 7 shows the stiffness curves for the different cases. As it could be predicted, stiffness slightly increases with the osculation ratio, since a more conformal contact is stiffer. *Rf* does not affect the stiffness as it does not change the contact geometry. A higher λ_r involves a larger wire diameter, which makes the wire ring contact stiffer. Finally, an increase in ball diameter leads to a more flexible bearing. This effect comes from the reduction of the number of rolling elements; a contact with a larger ball is stiffer but fewer contacts have to face to higher contact forces for the same external applied force.

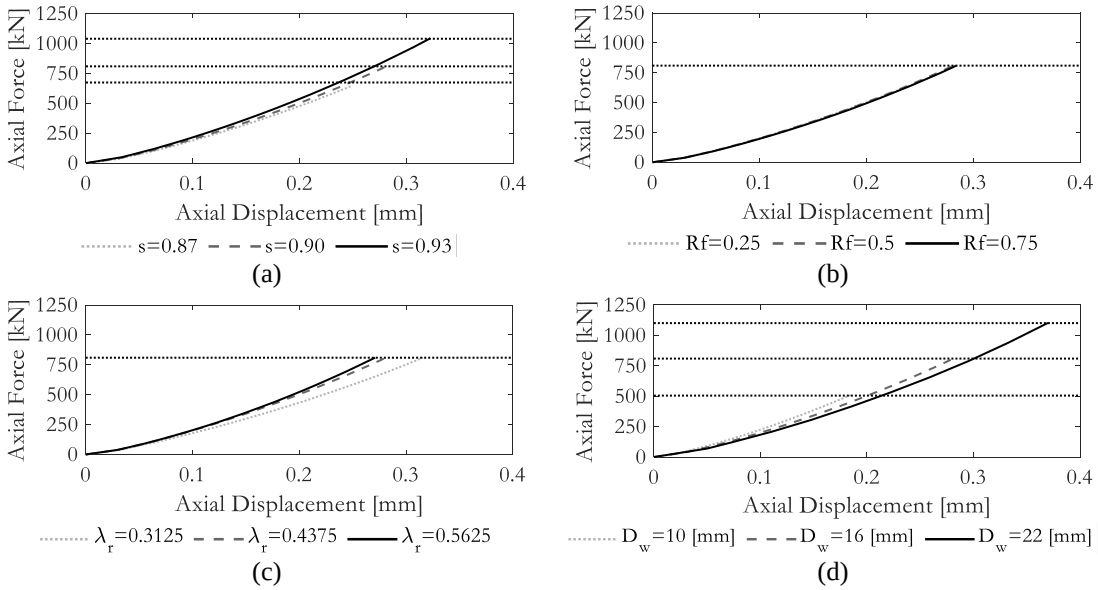

Fig. 7. Ball bearing stiffness results: (a) Osculation ratio (b) Race Factor (c) λ_r (d) Ball diameter

Wire Twist

Fig. 8 shows that larger osculation ratios lead wire twist to start earlier, because in a less conformal contact the ball would not climb so much over the raceway. Race factor almost does not affect wire twist; however a slight difference can be seen near C_{0a}. This phenomenon happens because larger *Rf* values involves larger raceways, favouring ball climbing and therefore more descentered contact ellipse that generates more wire twisting moment. The effect of increasing λ_r and D_w is the same since both of them modify the size of the housing (H). The smaller the size, the larger the wire twist for the same external applied displacement (Δ_{axial}) and vice versa, as it can be observed in Fig. 9, where (θ) is an angle related with the wire twist. Besides, it has been proved that the wire twist varies proportionally with the inverse of D_w.

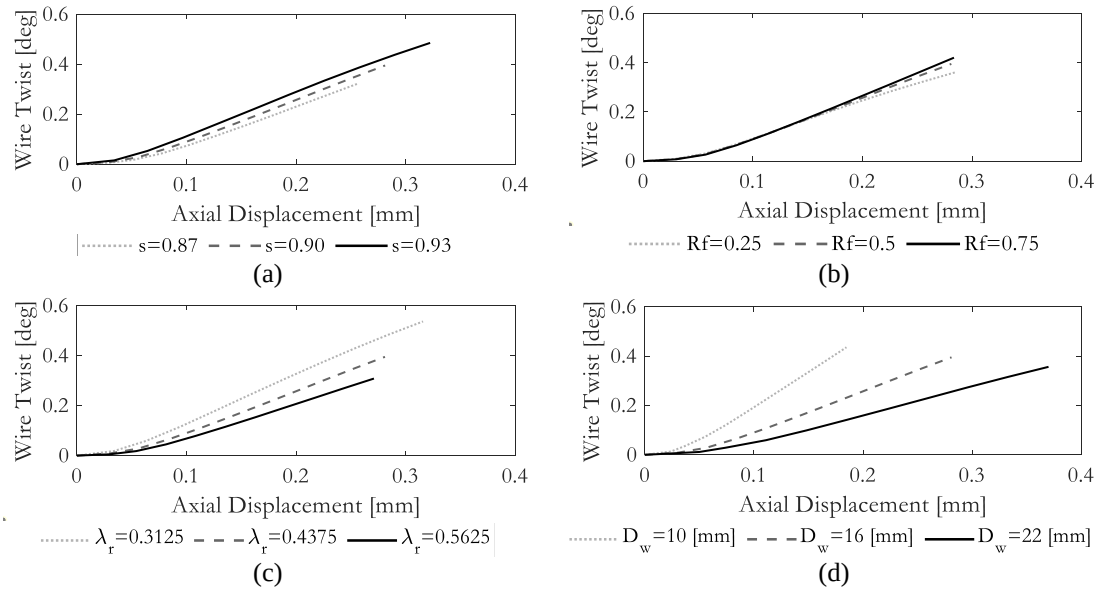

Fig. 8. Ball bearing wire twist results: (a) Osculation ratio (b) Race Factor (c) λ_r (d) Ball diameter

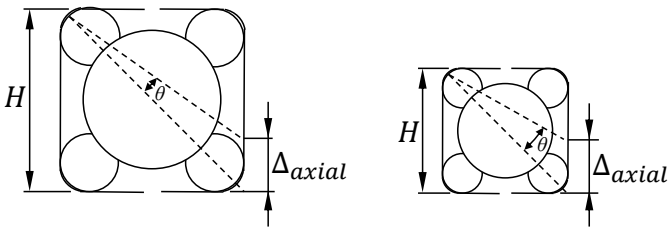

Fig. 9. Effect of an external applied displacement in wire twist

Contact Angle

Contact angle is related to wire twist and ball climbing phenomenon as it can be derived from plots in Fig. 8 and Fig. 10. As mentioned before, larger osculation ratios make the ball start to climb over the raceway at an early time and stabilizes later because of the action of the wire twist. Lower osculation ratios are less likely to climb over the raceway, for that reason the evolution of the curves is not so aggressive. The variation with *Rf* is similar at the beginning and suffer a later deviation because of the wire twist. The increasing wire twist with the reduction of λ_r keeps the contact ellipse centered at the raceway, which results in a pretty constant contact angle. D_w seems not to have almost effect on the contact angle, nevertheless for smaller values the ball tends to start climbing faster and rise the contact angle, which is later counterbalanced by the wire twist.

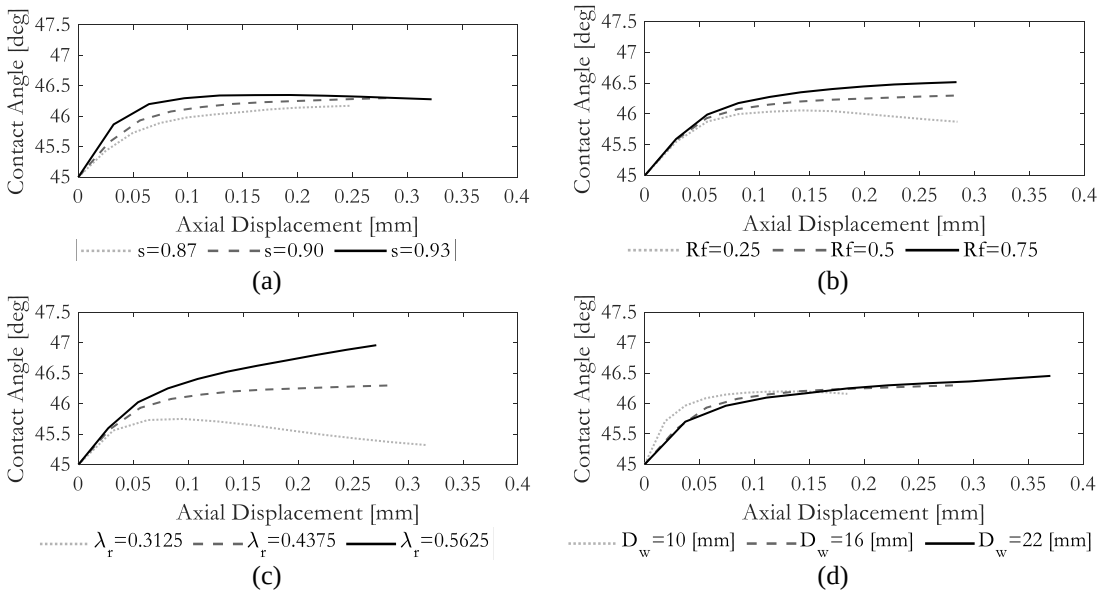

Fig. 10. Ball-wire contact angle results: (a) Osculation ratio (b) Race Factor (c) λ_r (d) Ball diameter

Contact Pressure Contours

These graphs are relevant since they indicate whether the maximum allowable load pressure has been exceeded or if the contact ellipse has reached the raceway boundaries causing truncation. Note that, in this case, truncation happens to be in the less loaded zone of the ellipse; for that reason, the pressure peaks are not as acute as it could be expected in the edges. Osculation ratio appears to generate the expected behaviour, that is, a more concentrated contact arises with lower values of the osculation ratio. The effect of reducing the raceway with large values of *Rf* or small values of λ_r increases the risk of suffering ellipse truncation as it can be observed in Fig. 11(b) and Fig. 11(c). As a result of varying the values of D_w, it can be stated that the behaviour of the contact ellipse is identical but scaled. Another conclusion that can be obtained from these graphs is that the static load capacity calculated in [16] seems to be a good estimate, and that truncation can be a problem with certain small values of *s*, *Rf* or λ_r.

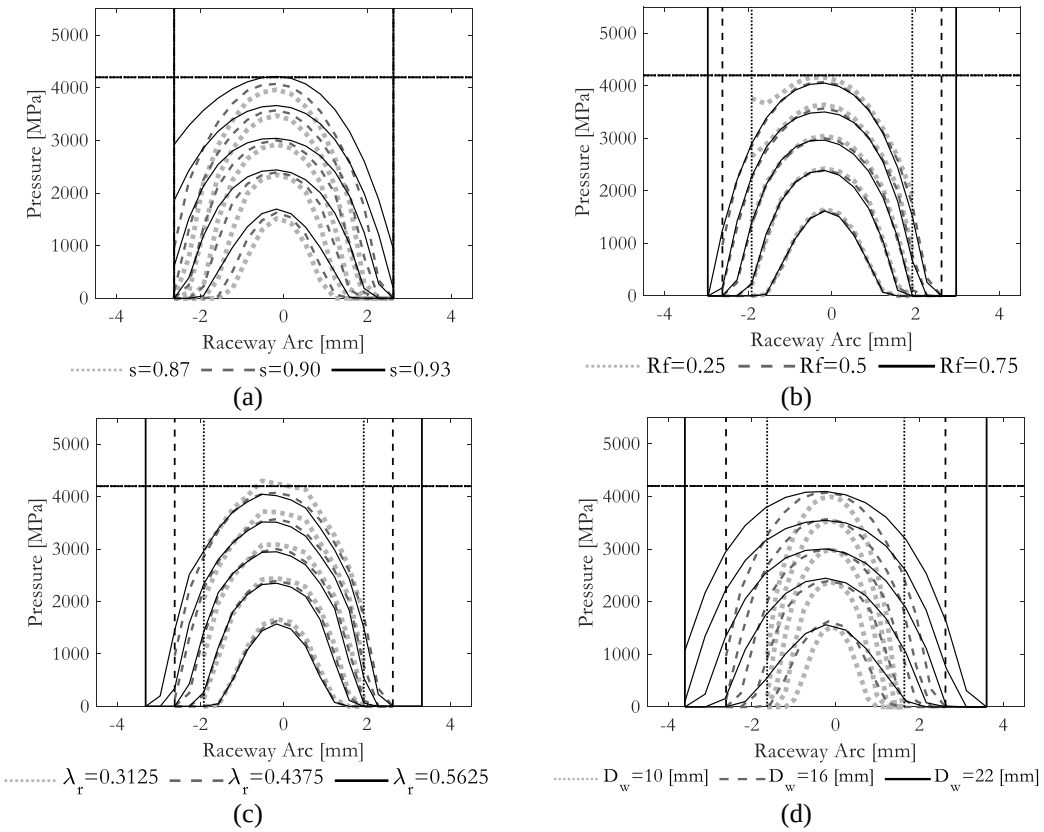

Fig. 11. Ball bearing contact pressure results: (a) Osculation ratio (b) Race Factor (c) λ_r (d) Ball diameter

3.2. Roller Bearings

Previous considerations

Fig. 12 shows a summary of the main and crossed effects of each geometrical parameter in the overall values of the performance indicators, where the summation of main and crossed effects equals 100%. The summation of crossed effects is equal or below 20% for all performance parameters, specifically 20% for axial static load capacity, 11% for stiffness, 14% for wire twist and 17% for contact angle. For that reason, it can be stated that the influence of crossed effects is low.

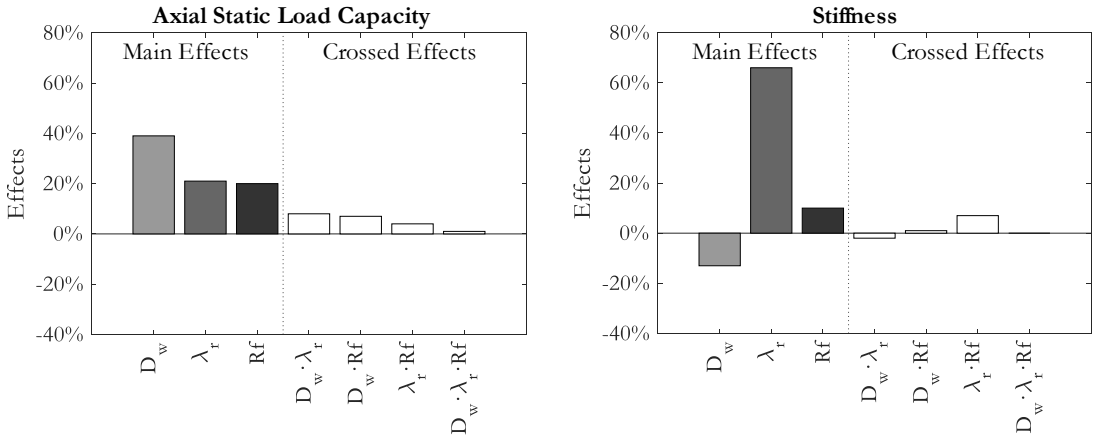

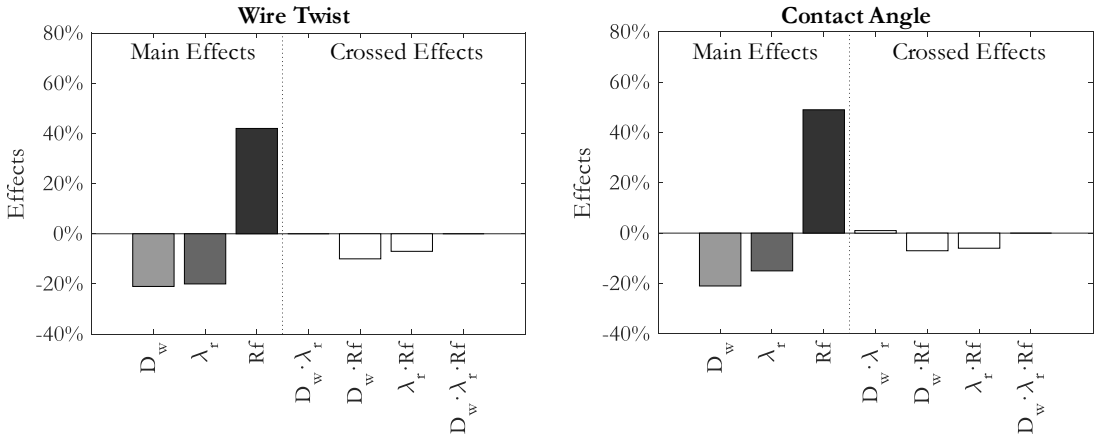

Fig. 12. Roller bearing main and crossed effects

Axial Static Load Capacity

This indicator depends on the contact geometry, and it is affected by all the studied parameters, because all of them modify the contact length. *Rf* and λ_r have fewer influence in C_{0a} compared with D_w.

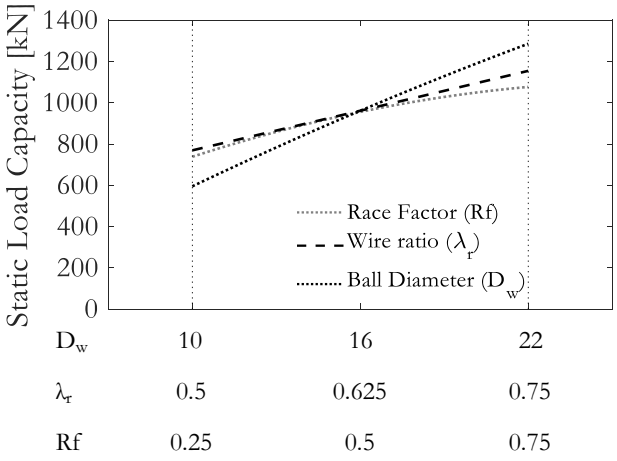

Fig. 13. Roller bearing static load capacity

Regarding the effect of varying D_w on the static load capacity, there is another important fact that must be pointed out. In the DoE arranged in this paper, the chosen design parameters are D_w, λ_r and *Rf*. But if the chosen parameters were D_w, λ and *Rf*, it is worth noting that if D_w varied maintaining λ and *Rf* constant, the axial capacity would be constant, and therefore an increment in D_w would not be a valid strategy to increase the load capacity. To prove this, consider the formula proposed in ISO-76 standard to obtain the static load capacity for conventional bearings (Eq. 3):

$$C_{0a} = 220 \cdot \left(1 - \frac{D_w \cdot \cos(\alpha)}{D_{pw}}\right) \cdot Z \cdot L_w \cdot D_w \cdot \sin(\alpha) \qquad (3)$$

In that case, if λ and *Rf* remained constant, so would do the contact length; additionally, for slewing bearings the term in parenthesis is close to one, and D_w is inversely proportional to the number of rollers (Z) with a constant fill ratio, which implies that an increment in one of them would cause a reduction in the other, maintaining the static load capacity constant.

Axial Stiffness

Axial stiffness is influenced by contact geometry: a roller raceway contact with larger contact length is stiffer than other with a smaller one, as it can be observed when *Rf* or λ_r increases. In terms of *Rf*, this phenomenon is non-linear since the relation between *Rf* and the raceway length is also non-linear. For that reason, the *Rf=0.25* curve is more flexible than the other two, where the contact length is similar. Roller

diameter seems to have little influence on axial stiffness; the effect of a more rigid contact with higher D_w is compensated with a fewer number of rollers.

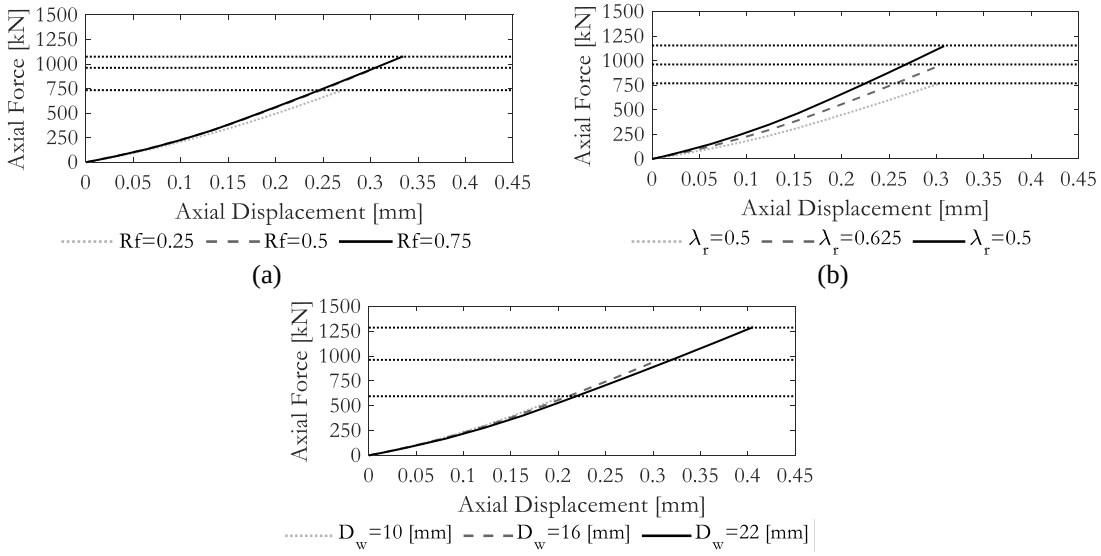

Fig. 14. Roller bearing stiffness results: (a) Race Factor (b) λ_r (c) Roller diameter

Wire Twist

As it happened with ball bearings, if the wire-roller-wire set is smaller, for the same applied external displacement the set can twist more. This comes from the compatibility of deformations [10]. This phenomenon can be observed in Fig. 15, where in every graph wire twist is larger when the roller-wires set is smaller.

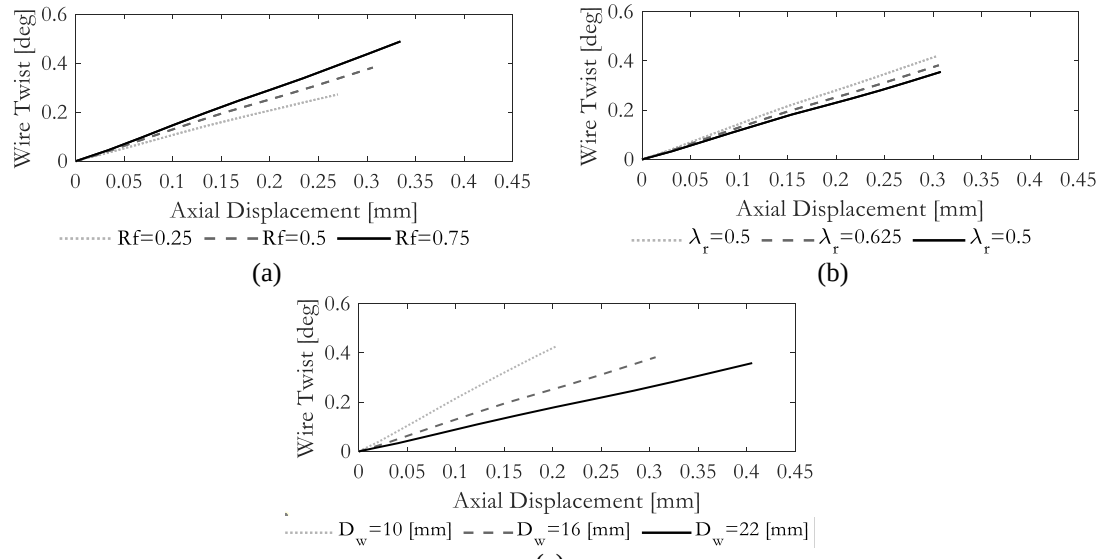

Fig. 15. Roller bearing wire twist results: (a) Race Factor (b) λ_r (c) Roller diameter

Contact Angle

Contact angle variation is so closely related to wire twist that the values of wire twist are almost the same values of contact angle variation. This small deviation comes from the deformation of the roller-wire contact.

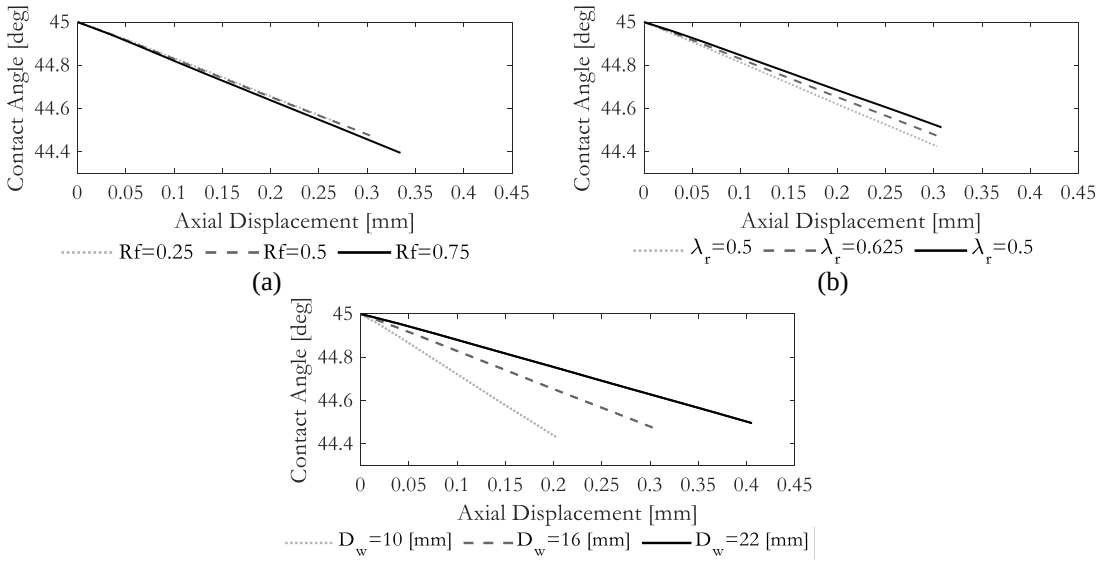

Fig. 16. Roller contact angle results: (a) Race Factor (b) λ_r (c) Roller diameter

Contact Pressure Contours

This section presents the pressure lines along the longitudinal axis of the contact patch during the loading process. In roller bearings the contact is always truncated in that axis; in this sense, even though very large non-realistic pressure peaks appear in Fig. 17 due to linear material assumption, this does not imply that those peaks do not exist. Indeed, the free edges of the wire exert some pressure peaks in the location of the wire edges. However, this pressure peaks can be avoided in a great extent with edge filleting and a slight crowning. Identical behaviour is observed in all cases, where friction generates a tangential force in roller-wire contact that tilt the pressure lines, making them surpass the maximum pressure. It is something that could be predicted, since the analytical model used to obtain the theoretical C_{0a} assumes that the contact angle remains constant at 45 [°].

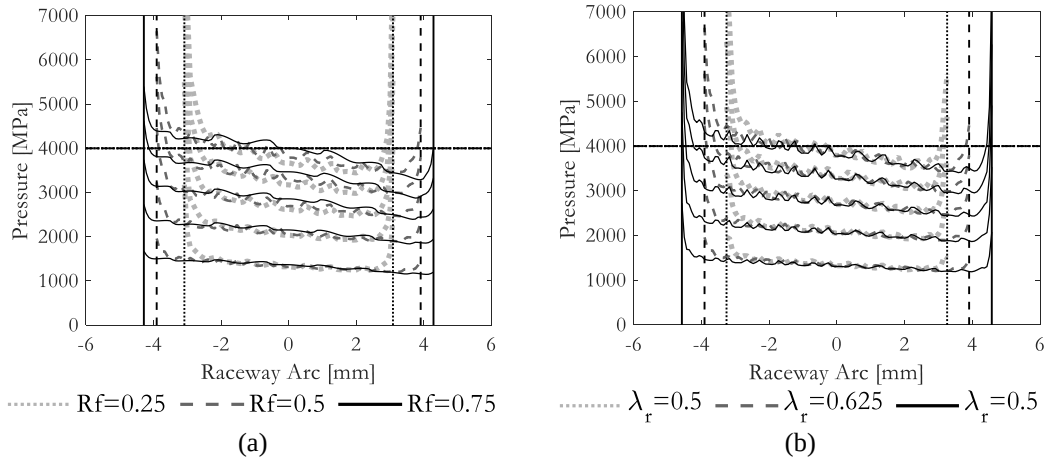

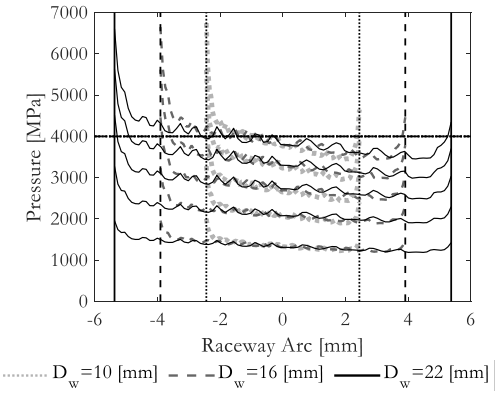

(c)

Fig. 17. Roller bearing contact pressure results: (a) Race Factor (b) λ_r (c) Roller diameter

3.3. Results Summary

All the results presented in this section are gathered in Fig. 18 for ball bearings and in Fig. 19 for roller bearings. These plots compare the overall performance indicators of the reference case with the ones where a single parameter was increased o decreased, providing a graphical idea of how much affects the variation of a geometrical parameter to the overall value of the performance indicator.

Ball bearings

Axial static load capacity is only affected by osculation ratio and ball diameter, with a significant variation. Overall stiffness constant retrieved a slight increase with high values of osculation ratio and λ_r and low values of ball diameter. Overall contact angle seems to increase with all studied parameters, especially with λ_r. Overall wire twist is not affected so much by studied parameters. Contact angle variation is not so closely related to wire twist since ball climbing phenomenon has a significant contribution. In addition, nonlinearities are observed for some design parameters on some performance indicators and the most evident ones are: the influence of the conformity on the axial load capacity, the influence of the nondimensional wire diameter on the stiffness, and the influence of the conformity and the race factor on the contact angle.

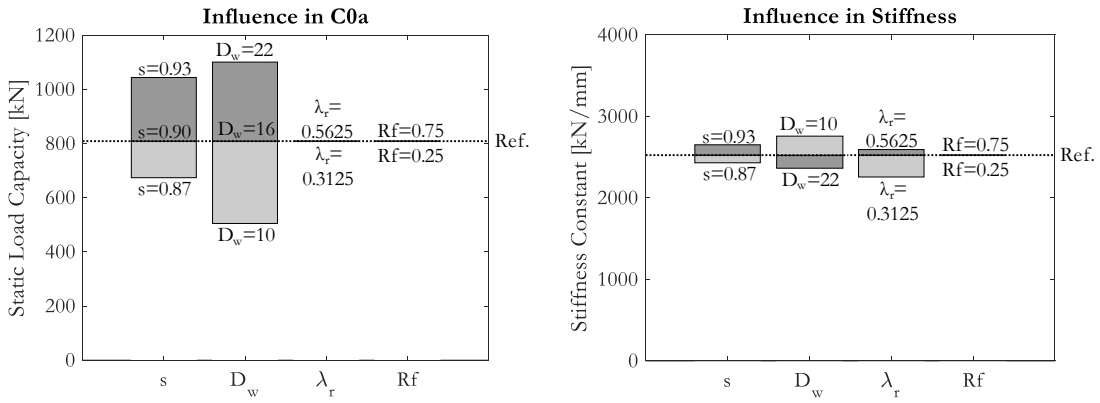

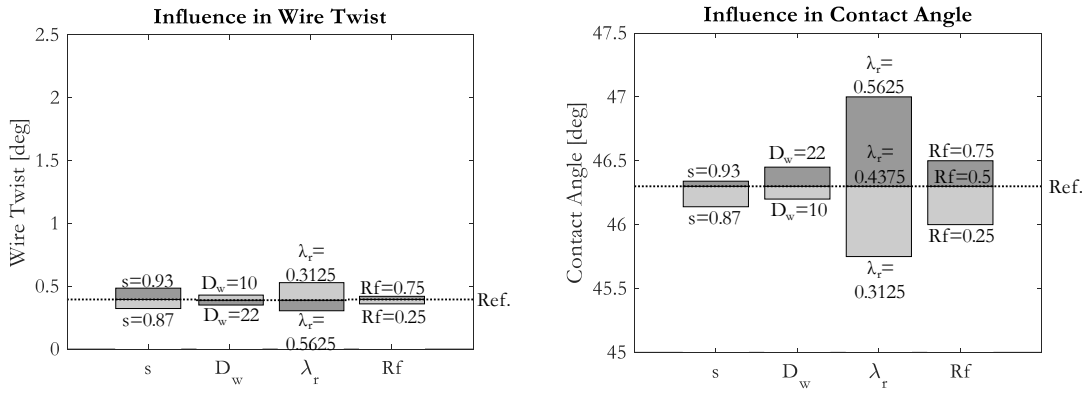

Fig. 18. Infuence of the design parameters in ball bearing performance

Roller bearings

Axial static load capacity suffer important variations with all geometrical parameters because of the contact length increment or decrement. On the one hand, stiffness does not change significantly with roller diameter because of the effect of increasing the contact length is compensated with the reduction in the roller number. On the other hand, λ_r and *Rf* affect directly to the geometry of the roller wire and wire-ring contacts which contribute to changes in stiffness. Variations in contact angle and wire twist are closely related with a little deviation caused by roller-wire contact deformation. In addition, nonlinearities are observed for some design parameters on some performance indicators and the most evident ones are: the influence of *Rf* on the axial load capacity and the stiffness, and the influence of the roller diameter on the wire twist.

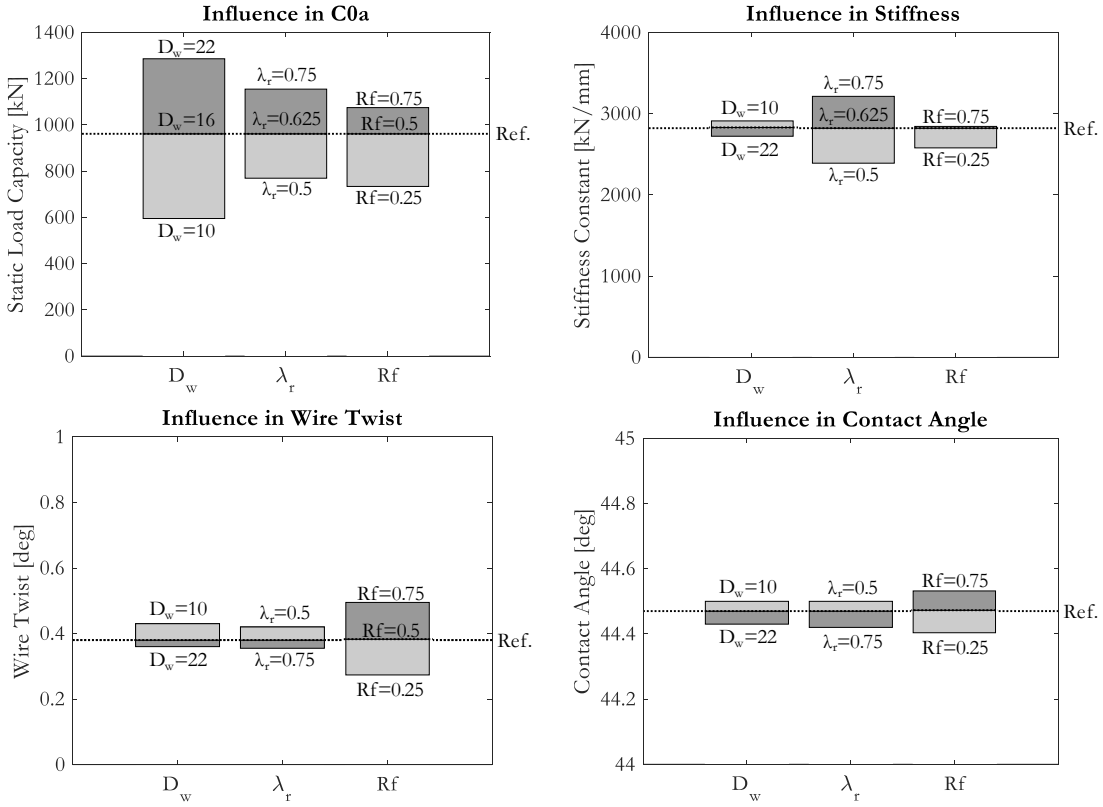

Fig. 19. Infuence of the design parameters in roller bearing performance

4. Conclusions

A study of the influence of the most important geometrical parameters in ball and crossed roller wire race bearings performance under axial load were carried out. The aim of this work was to provide some indications of how the structural behaviour varies with some design parameters such as rolling element diameter (D_w), osculation ratio (s), wire diameter to rolling element diameter ratio (λ_r) and raceway factor

(*Rf*). To achieve that, two Finite Element analysis campaings were performed and the results compared. The matrices of experiments were based on varying geometrical parameters from reference geometries obtained from commercial catalogues. Fig. 20 summarizes the influence of each design parameter on each performance indicator. The values in those figures are the variation percentages of the performance indicators when each design parameter increases from its minimum value to its maximum value in the DoE with respect to the minimum.

Regarding wire race ball bearings results, static load capacity is only affected by contact geometry parameters such as *s* and D_w. Axial bearing stiffness does not change significantly, increasing with *s* and λ_r and decreasing with D_w. Contact angle variation increases with all parameters but abruptly with λ_r. Wire twist increases with *s* and *Rf* and decreases with D_w and λ_r.

In the case of crossed roller wire race bearings, the static load capacity happens to increase with all design parameters. Axial bearing stiffness decreases slightly with D_w and rises with λ_r and *Rf*. Contact angle variation and wire twisting increase only with *Rf* and decrease with D_w and λ_r.

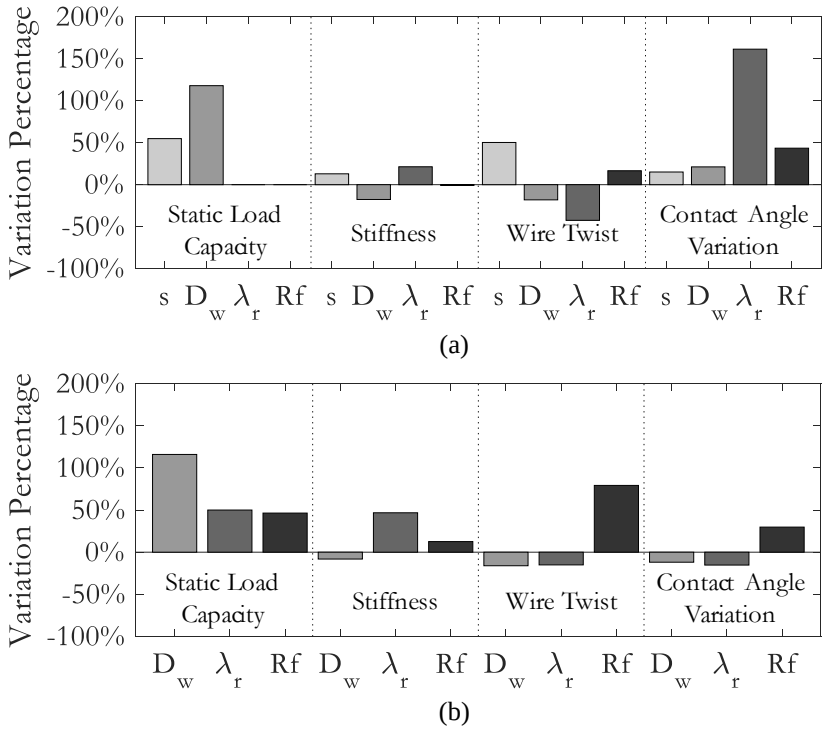

Fig. 20. Relative influence of geometrical parameters in performance: (a) Ball wire race bearings (b) Roller wire race bearings

Acknowledgements

The authors want to acknowledge the financial support of the Spanish Ministry of Economy and Competitiveness through grant number DPI2017-85487-R (AEI/FEDER,UE); the Basque Government through project number IT947-16 and research program HAZITEK 2019, acronym WIRE; and the University of the Basque Country through doctoral grant number PIF18/071.

Special thanks also to Basque manufacturer Iraundi Bearings S.A. for the help in many background items of the research.

References

[1] Franke Special Bearings Brochure: Light Bearings for Innovation 2015.

[2] Erde R. Rothe Erde wire-race bearings. The proven bearing concept. n.d.

[3] SKF. SKF WireRace and inserted raceway bearings for weight savings and consistent friction torque Brochure 2018.

[4] Gunia D, Smolnicki T. The Influence of the Geometrical Parameters for Stress Distribution in Wire Raceway Slewing Bearing. Arch Mech Eng 2017;64. https://doi.org/10.1515/meceng-2017-0019.

[5] Gunia D, Smolnicki T. Comparison of Stress Distribution Between Geometrically Corrected Wire-Raceway Bearings and Non-corrected Wire-Raceway Bearings. In: Rusiński E, Pietrusiak D, editors. Proc. 14th Int. Sci. Conf. Comput. Aided Eng., Cham: Springer International Publishing; 2019, p. 266–75.

[6] Martín I, Heras I, Aguirrebeitia J, Abasolo M, Coria I. Static structural behaviour of wire bearings under axial load: Comparison with conventional bearings and study of design and operational parameters. Mech Mach Theory 2019;132:98–107. https://doi.org/10.1016/J.MECHMACHTHEORY.2018.10.016.

[7] Shan X, Xie T, Chen W. A new method for determining the preload in a wire race ball bearing. Tribol Int 2007;40:869–75. https://doi.org/https://doi.org/10.1016/j.triboint.2006.09.003.

[8] Aguirrebeitia J, Martín I, Heras I, Abasolo M, Coria I. Wire twisting stiffness modelling with application in wire race ball bearings . Derivation of analytical formula and finite element validation. Mech Mach Theory 2019;140:1–9. https://doi.org/10.1016/j.mechmachtheory.2019.05.012.

[9] Martín I, Heras I, Aguirrebeitia J, Abasolo M, Coria I. Analytical Model for the Estimation of Axial Stiffness and Contact Results in Wire Race Ball Bearings. In: Uhl T, editor. Adv. Mech. Mach. Sci. Proc. 15th IFToMM World Congr. Mech. Mach. Sci., Cham: Springer International Publishing; 2019, p. 3873–82.

[10] Martín I, Heras I, Coria I, Abasolo M, Aguirrebeitia J. Structural modeling of crossed roller wire race bearings: Analytical submodel for the roller-wire-ring set. Tribol Int 2020:106420. https://doi.org/https://doi.org/10.1016/j.triboint.2020.106420.

[11] Heras I, Aguirrebeitia J, Abasolo M, Coria I. An engineering approach for the estimation of slewing bearing stiffness in wind turbine generators. Wind Energy 2019;22:376–91. https://doi.org/10.1002/we.2292.

[12] KMF. Wire race ball bearings product catalogue n.d.

[13] Joshi A, Kachhia B, Kikkari H, Sridhar M, Nelias D. Running Torque of Slow Speed Two-Point and Four-Point Contact Bearings. Lubricants 2015. https://doi.org/10.3390/lubricants3020181.

[14] Gonçalves D, Pinho S, Graça B, Campos A V., Seabra JHO. Friction torque in thrust ball bearings lubricated with polymer greases of different thickener content. Tribol Int 2016. https://doi.org/10.1016/j.triboint.2015.12.017.

[15] Heras I, Coria I, Aguirrebeitia J, Abasolo M. Par de fricción en rodamientos de vuelco de cuatro puntos de contacto: procedimiento de cálculo y resultados experimentales. XXII Congr. Nac. Ing. Mecánica, 19-21 Sept., Madrid, Spain: 2018.

[16] Aguirrebeitia J, Plaza J, Abasolo M, Vallejo J. Effect of the preload in the general static load-carrying capacity of four-contact-point slewing bearings for wind turbine generators: theoretical model and finite element calculations. Wind Energy 2014;17:1605–21. https://doi.org/10.1002/we.1656.

[17] Aguirrebeitia J, Abasolo M, Avilés R, Fernández de Bustos I. General Static Load Capacity in Slewing Bearings. Unified Theoretical Approach for Crossed Roller Bearings and Four Contact Point Angular Ball Bearings . 13th World Congr Mech Mach Sci 19-25 June 2011:19–25.

[18] ISO 76:2006. Rolling bearings - Static load ratings. 2006.